Nonlinear Interactions Generating Wave-4 Terdiurnal Tides, TE1 and TW4: A Comparison of ICON Observations and SD-WACCM-X | Rythm Agarwal, Scott L. England, Guiping Liu

1. Background, Introduction and Motivation

What are tides and planetary waves?

These are global scale wave-like disturbances in winds and temperature in the MLT region that generate at lower altitudes and propagate upwards, causing changes in the ion production, loss and transport. They are caused by solar heating, in combination with processes such as cloud formation, and have a lot of variability year round and under all geophysical conditions. Tides can also be produced in the thermosphere by absorption of solar radiation, and by wave-wave interactions involving tides and planetary waves. Tides can interact with one another and create more tides, thus making the simulation of atmospheric layers more complex and necessary.

Significance of atmospheric tides

- Potential drivers of ionospheric variability originating from the troposphere and stratosphere.
- They create a dynamo effect with the electric fields between altitudes 100-300 km, thus significantly influencing the plasma distribution in the ionosphere.
- They redistribute solar energy between different atmospheric layers.
- Key characteristics for studying atmosphere-space coupling of Earth and other planets.

Tidal Harmonics:

Temporal period: n = [1,3] - signify 24 (Diurnal), 12 (Semidiurnal) and 8 (Terdiurnal) hour period respectively.
Zonal wavenumber: s = [-6,6]; When n = 0, they are called Stationary Planetary Waves (SPWs). Migrating tides refer to a same (n,s) pair such as (3,3). When s < 0, the tides are Eastward and when s > 0, they are Westward propagating.

What are the missing pieces that this research is tending to?

- Many studies highlighted that non-migrating tides are much larger in the MLT region with a focus on diurnal and semidiurnal tides, it was required to look at the same for terdiurnal tides in both E- and F-region.
- Since terdiurnal tides remain poorly characterized due to their overall weaker presence in the atmosphere, this study provides a deeper insight into the wave-4 terdiurnal tides.
- Understanding whether nonlinear interactions generate upper atmospheric terdiurnal tides, TE1 and TW4.
- Observing 4 nonlinear interactions: SPW4×TW3 →TE1, DE3×SW2 →TE1, DW2×SW2 →TW4, SPW1×TW3 →TW4 with ICON, and validating with SD-WACCM-X model results.

2. Data Sources and Instrumentation

Ionospheric Connection, ICON, explorer performs a scientific investigation to understand the fundamental question of atmosphere-ionosphere coupling. Through magnetically connected remote and in-situ measurements, ICON measures quantities such as neutral wind, temperature and ion density profiles. The explorer has an instrument on board - **Michelson Interferometer for Global High-resolution Thermospheric Imaging, MIGHTI**, that provides limb observations of altitude profiles of the mentioned quantities during day and night time. This instrument is dedicated to address the science question of the ICON mission to identify the source of strong ionospheric variability.

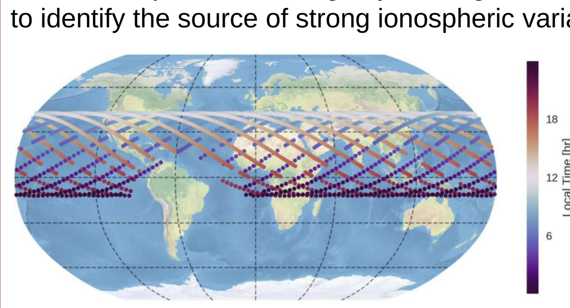

Fig. 1: Geographic coverage of MIGHTI observations, after Englert et al. 2017a; Harding et al. 2017a.

Data characteristics used in the study for ICON:

- Latitudes: 5-40° N
- Altitude: 100.14 km (Actual altitude is ~100-103 km; Green line) and 253.71 km (Actual altitude is ~253-263 km; red line)
- Dates: Dec 2019 – Sep 2022

Specified Dynamics-Whole Atmosphere Community Climate Model with Thermosphere and Ionosphere Extension, SD-WACCM-X, is a comprehensive numerical model that simulates the Earth's atmosphere, spanning from its surface all the way up into the upper atmosphere. **The –X (eXtended)** indicates that the model has been pushed to higher altitudes to include the ionosphere, which essentially enables the study of space weather and geosphere coupling. The **Specifies Dynamics** is a configuration mode where the wind and temperature fields in the lower and middle atmosphere are constrained by the real-world observational weather data.
For this study, the sampled model, is referred to a portion of the model measured on the ICON Local Time- Longitude grid.

- Latitudes: 12° S - 42° N; Selected range- 5-40° N
- Altitude: 90-300 km; Selected levels - 100 km and 250 km
- Dates: Jan 2020 – Sep 2022

ICON sampling on the full SD-WACCM-X:

The full SD-WACCM-X has a longitude coverage at all local times. Figure 2 shows two plots which show how the data is spread in each of our binned data sections. Figure 2b highlights more evidently how uneven is the longitude coverage by the local time.

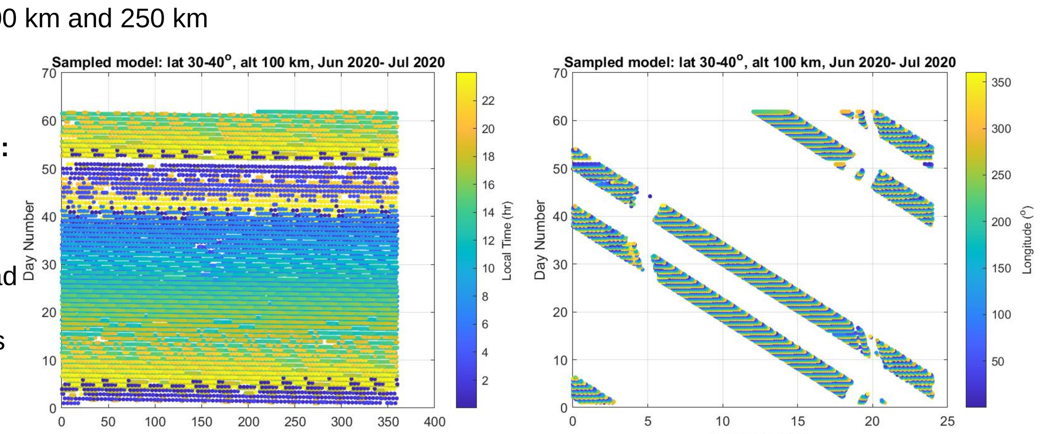

Fig. 2 (a, b): Data points coverage in SD-WACCM-X during Jun-Jul 2020 at 30-40° lat, 100 km after ICON sampling. (a) is on Day Number vs Longitude and (b) is on Day Number vs Local Time.

3. Tidal Modelling and Analytical Methods

Data Processing – Wave Model, Tide Fitting and Reconstruction

- We applied multiple levels of processing the data, first of which is eliminating the flagged values, averaging the data set into 60-day bins with a step size of 30 days and 10° latitude bins (0°-45° N).
- Then, the entire data set is fit to the wave model considered for this study. First, migrating tides and SPWs are fit on the UT and Longitude grid as the model is tailored to those as shown in Equation 1. For the SPWs, *n=0* and *s = [0,4]*. Secondly, the resulting amplitudes are subtracted from the dataset and the residuals are then fit through the model containing nonmigrating tidal harmonics as shown in Equation 2. Here, $|s-n| \le 4$ (wave-4 configuration) and $i \neq j$.

$$A_0 + B_0 + \sum_{i=1}^{3}\sum_{j=1}^{3}\left(A_{ij}\cos\left(n_i t\frac{2\pi}{24} + s_j\lambda\frac{2\pi}{360}\right)\right) + \left(B_{ij}\sin\left(n_i t\frac{2\pi}{24} + s_j\lambda\frac{2\pi}{360}\right)\right) - \phi_i \quad \text{[Eq. 1]}$$

$$\sum_{i=1}^{3}\sum_{j=-3}^{7}\left(A_{ij}\cos\left(n_i t\frac{2\pi}{24} + (s_j-n_i)\lambda\frac{2\pi}{360}\right)\right) + \left(B_{ij}\sin\left(n_i t\frac{2\pi}{24} + (s_j-n_i)\lambda\frac{2\pi}{360}\right)\right) - \phi_i \quad \text{[Eq. 2]}$$

- Further, from the output of the fit, uncertainties for the amplitudes are calculated using a standard least-squares uncertainty propagation from the sine/cosine coefficients into the amplitude.

$$\sigma_A = \sqrt{2}\,\frac{\sqrt{a^2\sigma_a + b^2\sigma_b}}{A} \quad \text{[Eq. 3]}$$

- The desired results from MIGHTI, ICON are shown as amplitude heatmaps on Latitude vs Day Of Year (DOY) and also shown are line plots of yearly latitudinal patterns of the tides in sections 4 and 5 respectively.
- Lastly, a correlation analyses is performed whose results are displayed in section 6.

Nonlinear Interaction of Wave-4 Tides

$$\underbrace{\cos(4\lambda)}_{\text{SPW4}}\underbrace{\cos(3\Omega t + 3\lambda)}_{\text{TW3}} \rightarrow \underbrace{\cos(3\Omega t - \lambda)}_{\text{TE1}} + \underbrace{\cos(3\Omega t + 7\lambda)}_{\text{TW7}} \quad \text{[Eq. 4]}$$

Equation 4 represents the interaction of two primary waves resulting in the in-situ generation of two secondary waves. The four nonlinear interactions presented in this study are derived from this framework. Only one of the two secondary waves are shown.

4. Nonlinear Interaction Observations from ICON Temperatures at 100 km

This section uses our tidal analyses results on the ICON dataset to view possible nonlinear interactions between two primary waves, which result in secondary terdiurnal waves. We look at two interactions forming TE1 and TW4 each. Here, temperature amplitude plots on a Latitude vs DOY grid at 100.14 km are shown through a node diagram where each colored arrow indicates one of the following nonlinear wave-wave interactions:

SPW4 × TW3 → TE1 + TW7
DE3 × SW2 → TE1 + DW5
DW2 × SW2 → TW4 + D0
SPW1 × TW3 → TW4 + TW2

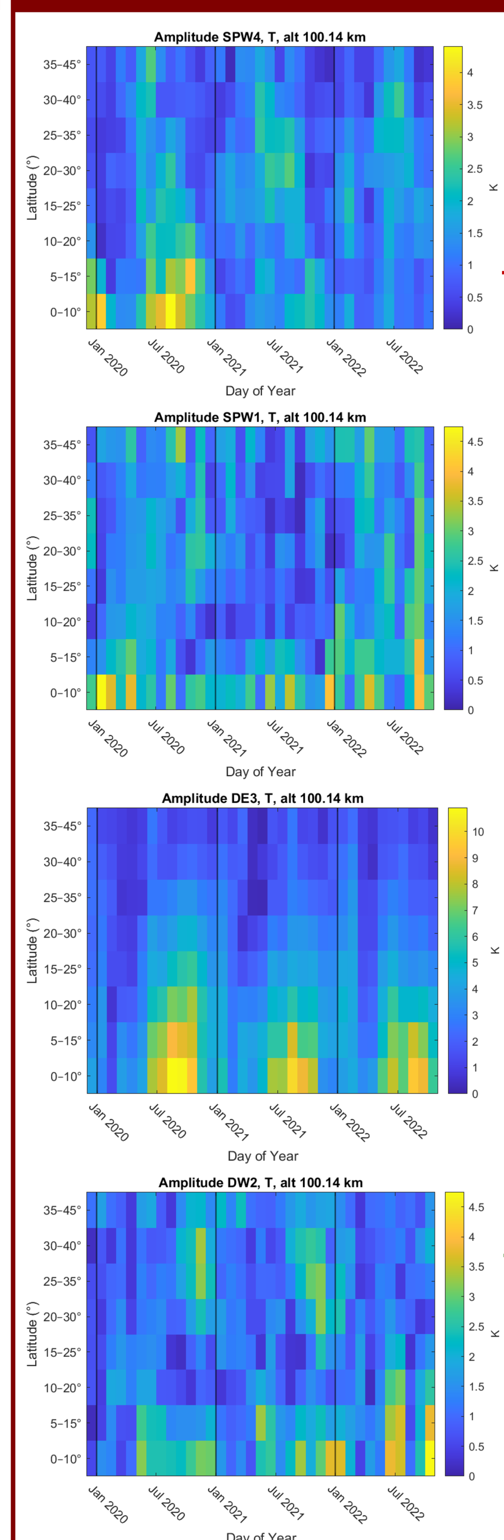

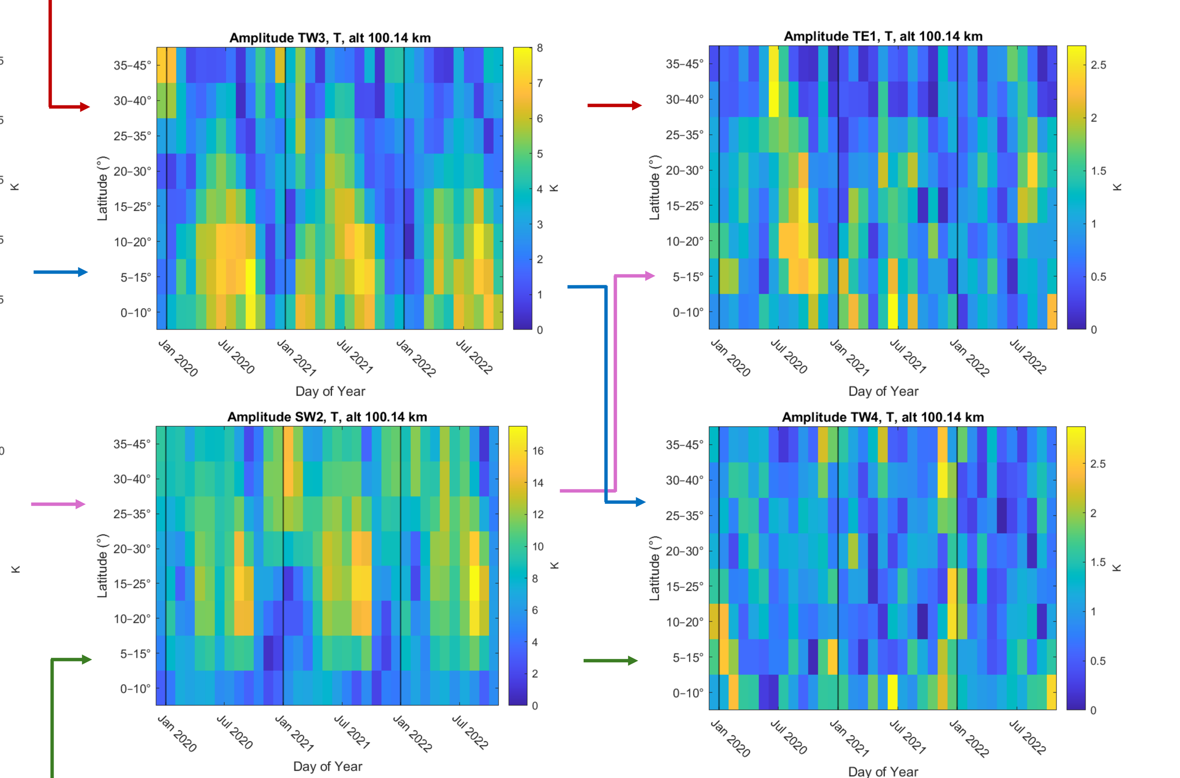

Fig. 3 (a - h): ICON Temperature amplitudes at 100.14 km on Lat vs DOY. (a-d) Left panel, top to bottom are tides and waves SPW4, SPW1, DE3, DW2; (e-f) Middle row, top to bottom are tides TW3 and SW2; (g-h) Right row, top to bottom are tides TE1, TW4.

- TW3, SW2, and DE3 show strong recurring seasonal enhancements and represent the most energetic waves among the candidate parent-wave pairs.
- TE1 and TW4 exhibit substantially smaller amplitudes than the proposed parent waves, consistent with their interpretation as secondary products of nonlinear interactions.
- The relatively weak and diffuse signatures of TE1 and TW4 prevent a clear identification of their sources from amplitude plots alone and they may also be falling in the range of noise levels, which is why weaker terdiurnal tides are harder to extract.

5. Yearly Latitudinal Patterns from ICON and Sampled SD-WACCM-X

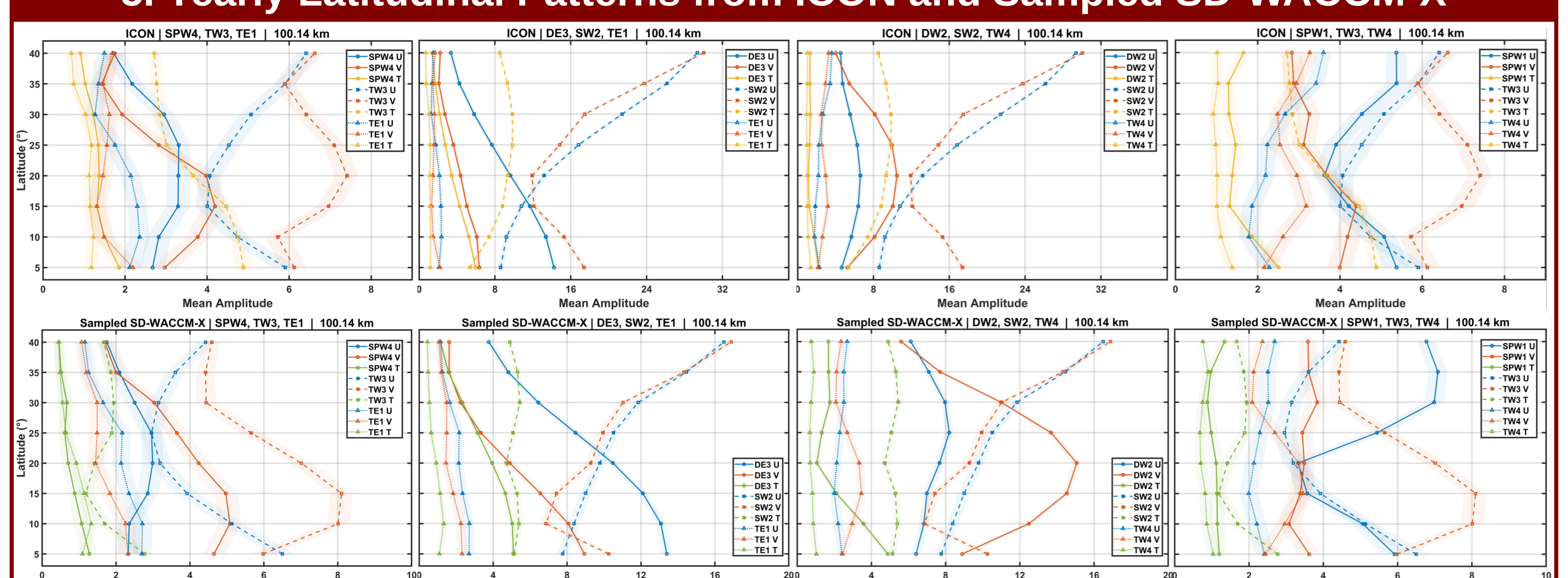

Fig. 4 (a-h): Annual Mean line plots with overlayed T,U,V at 100.14 km for each interaction. The uncertainty upto 1 std is also shown. (a-d) Top row, left-right are ICON and (e-h), Bottom row, left-right are Sampled SD-WACCM-X.

- 1st interaction shows local minima/maxima of zonal winds (U) closely tied to each other in both datasets, which indicate a probability of their interaction.
- T,U,V sharing similar latitudinal pattern for DE3 and TE1 in both datasets highlight a similarity in wave patterns in the 2nd interaction.
- T patterns for TW4 and DW2 are quite similar, more so in ICON than in the model for the 3rd interaction. The same is also visible in the 4th interaction with TW4 and SPW1.
- In the 4th interaction, the U, V patterns show a similar structure in both datasets, which suggests that the model is validating patterns picked up by ICON.

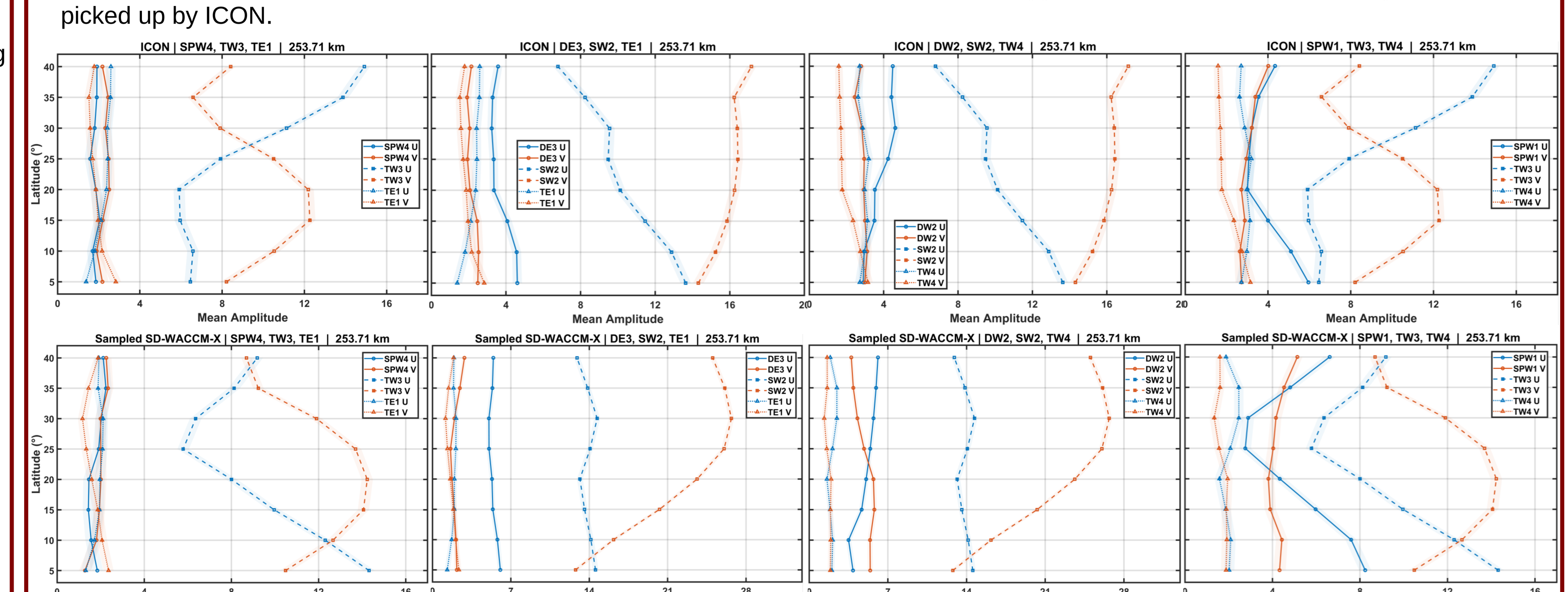

Fig. 5 (a-h): Annual Mean line plots with overlayed U,V at 253.71 km for each interaction. The uncertainty upto 1 std is also shown. (a-d) Top row, left-right are ICON and (e-h), Bottom row, left-right are Sampled SD-WACCM-X.

- In the F-region altitudes, except in the 1st interaction, the model shows a higher agreement in the latitudinal patterns of U between the primary waves.
- The amplitudes of the nonmigrating tide and/or the SPW parent wave and the secondary wave are similar in all of the interactions which suggest that for the higher altitudes, these tides may play an effective role to determine the amplitudes of the secondary wave.
- However, it is not clear how impactful are the migrating tides in this interaction at the higher altitudes.

6. Correlation Plots, Sectional Means, Sectional Mean Ratios

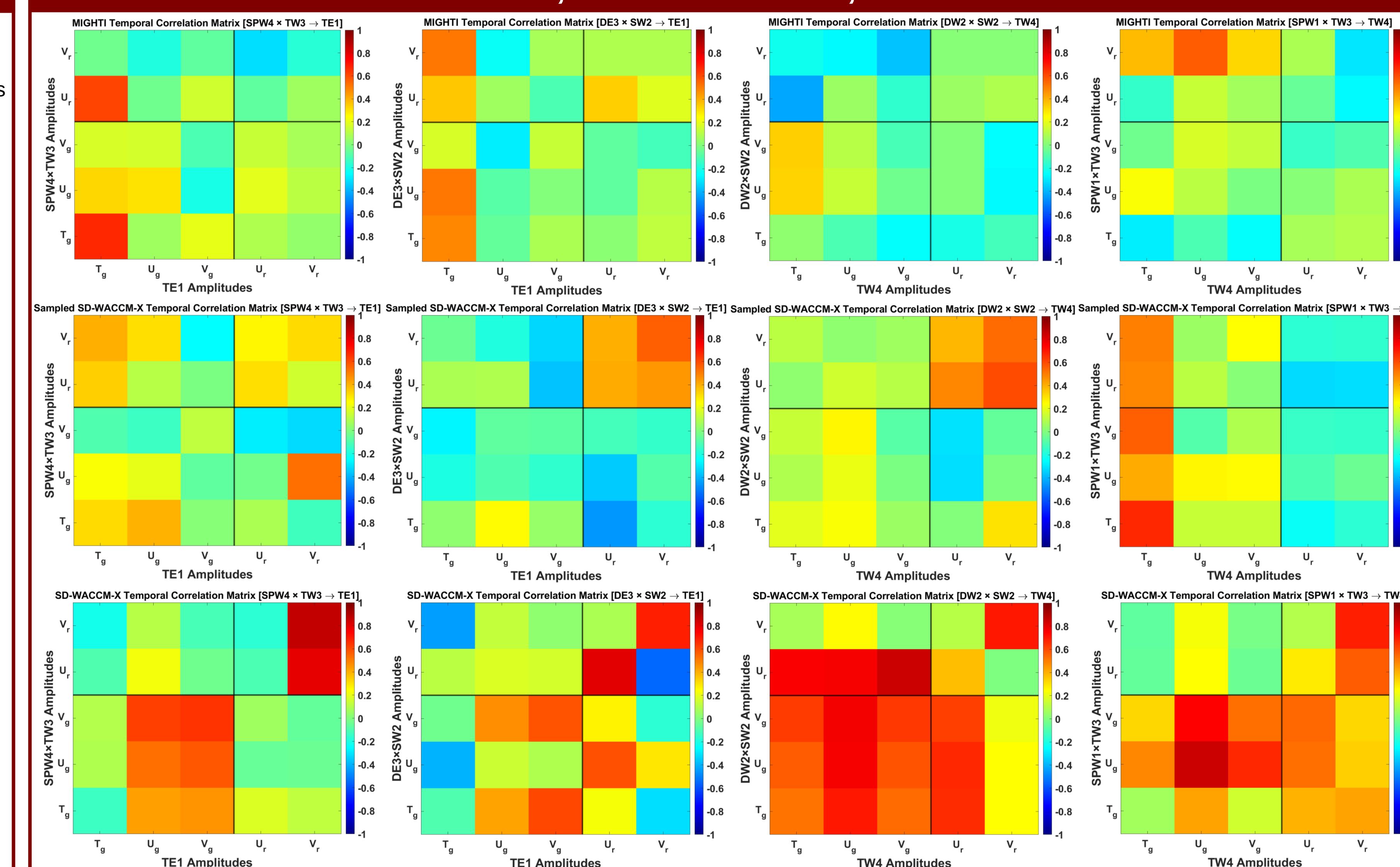

Fig. 6 (a - l): Correlation plots between T,U,V green line and U,V red line for all interactions. Y-axis has a combined amplitude of the primary waves and the x-axis represents the secondary waves; (a-d) Top row is ICON; (e-h) Middle row is Sampled Model; (i-l) Bottom row is Full Model

- These are correlation plots between the combined amplitudes of the primary waves and the secondary waves. These plots provide a way to visualize which variables in which regions have a high correlation which would provide evidence for the nonlinear interaction between them.
- In the ICON plots, T values in the E-region for 1st two interactions have a higher correlation which suggests that TE1 is a result of the interaction between SPW4 × TW3 and DE3 × SW2.
- U in the E-region also has a higher correlation than V. F-region doesn't not support any high values of correlations.
- The sampled model shows an opposite result for the 2nd and 3rd interactions where the complete F-region has a very high correlation which implies that U and V are interacting at higher altitudes and generating the respective secondary waves.
- The full model has many dominant regions with high correlations which directly support our argument that these nonlinear interactions are occurring.

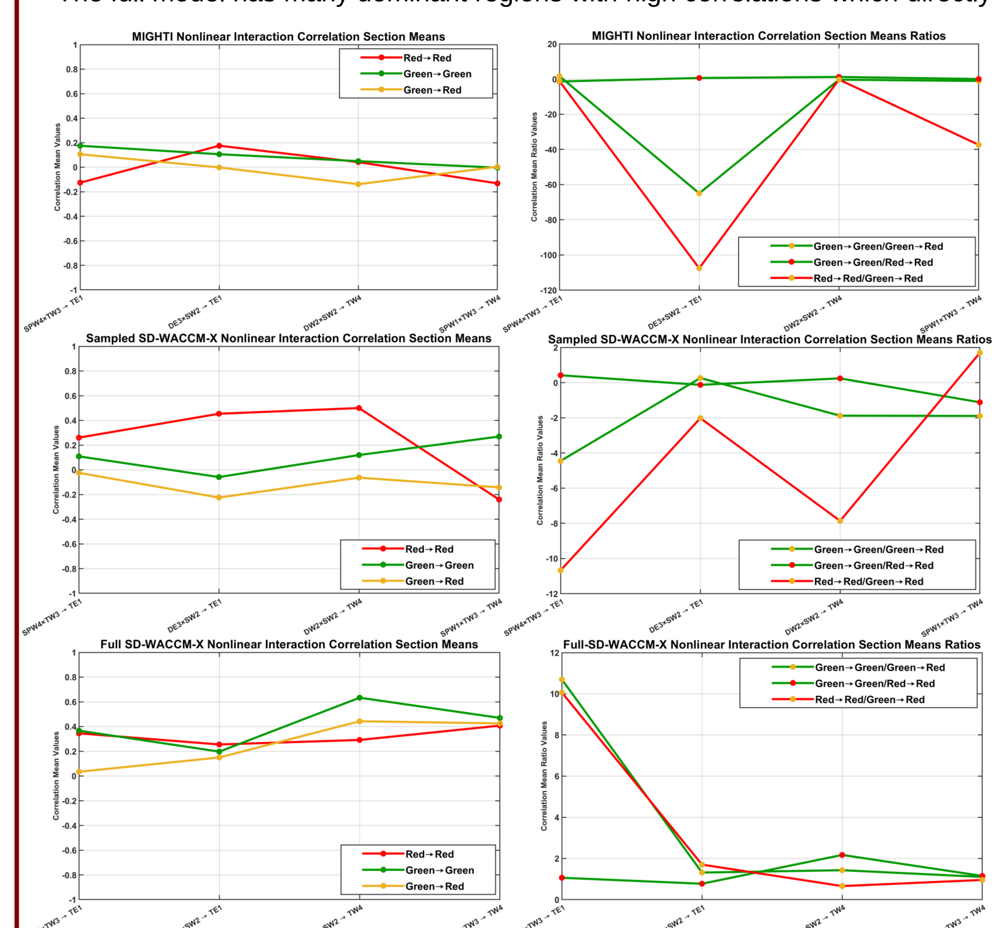

Table 1: Regional Mean Correlations Characteristics of Proposed Nonlinear Interactions

Wave-4 Nonlinear Interactions	Correlation Sections Means			ICON vs Sampled Model	ICON vs Full Model	Sampled Model vs Full Model	Agreement for all 3 models
	ICON	Sampled	Full				
SPW4×TW3→TE1				0, False	1, Partial	1, Partial	0, False
DE2×SW2→TE1				3, True	3, True	3, True	3, True
DW2×SW2→TW4				1, Partial	1, Partial	0, False	0, False
SPW1×TW3→TW4				1, Partial	1, Partial	3. True	1, Partial

Table 2: Cross-Dataset Trend Agreement for Nonlinear Interaction Ratios

Wave-4 Nonlinear Interactions	ICON	Sampled	Full	ICON vs Sampled % Match	ICON vs Full % Match	Sampled vs Full % Match	All three % Match
Green→Green / Red→Red	++-	-+-	-+-	66.67	66.67	100	66.67
Green→Green / Green→Red	-+-	+-0	-+-	0	100	0	0
Red→Red / Green→Red	-+-	+-+	--+	0	33.33	66.67	0

In synthesis, the table demonstrates Model agreement, Evident Sampling Effect, Weak Agreement for each row respectively.

Fig. 7 (a - f): (a-c) left column, top to bottom, are correlation sectional means for ICON, Sampled model and Full model; (d-f) right column, top to bottom, are correlation sectional means ratios

- Correlation section means provide an indicator which tells whether there is a larger agreement or disagreement in correlations of the complete region. Higher positive values indicate that in that particular section, the interaction appears spatially robust and there is a strong agreement. Lower positive values are indicative of existing interaction, but maybe not in the complete region evidently.
- Table 1 summarizes that among the 3 datasets, DE2×SW2→TE1 interaction has higher correlations in the F-region, lower in the E-region and lowest between the winds interacting in the E-region and propagating to the F-region to generate TE1.
- SPW1×TW3→TW4 interaction has only a partial agreement between all the comparisons which suggests that the Red line has the lowest correlation; i.e. it is not very likely that SPW1 and TW3 are interacting in the high altitudes to generate TW4.

- In Table 2, row 1, sampled model and the full model identify exactly the same ordering of the strength of the interaction between E- and F-region. Both the datasets show that correlation strength between green and red line peak for DW2×SW2→TW4 interaction. ICON reproduces most of this result.
- From row 2, ICON and the full model share exactly the same order of the strength of correlation between the tides in the E-region and the ones propagating to the F-region. This highlights that the model successfully represented what the satellite was capturing, but sampling the model distorted the results.
- For the row 3 ratio metric, the trend agreement is weak overall, which indicates that the spatial distribution of the correlations between the secondary wave generation in the F-region and the propagation of tides to the F-region is sensitive to both model formulation and sampling effects.

7. Conclusion and Future Work

- Correlation and pattern analyses provide evidence that nonlinear wave-wave interactions contribute to the generation of upper-atmospheric terdiurnal tides, with **DE3×SW2 → TE1** showing the strongest support across datasets.
- Comparisons between ICON observations and SD-WACCM-X indicate that several interaction signatures are reproducible, while others are strongly affected by observational sampling.
- TE1 exhibits more robust nonlinear interaction signatures than TW4, highlighting the need for further investigation of TW4 generation mechanisms and sampling impacts.
- Extend the analysis to multiple years and additional altitude levels to evaluate the seasonal, interannual, and vertical variability of nonlinear tidal interactions.
- Further investigate sampling effects and TW4 generation processes using targeted SD-WACCM-X simulations and additional observational constraints.
- This work was supported by NASA GSFC through grant # 80NSSC25K7856

CONTACT INFORMATION | Email: rythmagarwal@vt.edu